

**Military Technical College
Kobry El-Kobbah,
Cairo, Egypt.**



**13th International Conference
on Applied Mechanics and
Mechanical Engineering.**

SIMULATION OF A REVERSE OSMOSIS SEAWATER DESALINATION PLANT, PART 1: THEORETICAL MODELING OF A REAL PLANT AND ITS VALIDATION

SEOUDY*A., LOTFY* A.H. and SALEH* I.

ABSTRACT

The present work presents a theoretical modeling of a real reverse osmosis (RO) plant from the hydrodynamic point of view. Mathematical models for all elements of the plant have been developed including; booster pump; hydraulic filters; axial piston pump (high pressure pump); RO membranes; hydraulic accumulator; reject header, and throttling valve. These models have been simulated using SIMULINK 4 in MATLAB 6.1 environment. The pressure fluctuations of the axial piston pump have been determined theoretically with and without using hydraulic accumulator in the plant system at different flowrates and at different seawater salinities. Theoretical investigations have been performed to predict the dynamic characteristics of the plant axial piston pump and the RO membrane performance under normal and abnormal operating conditions. Experimental investigations have been introduced in part 2 of this paper to verify the theoretical model. The verified simulation model has been used to present a proposed operational chart for the investigated desalination plant in case of working under different seawater salinities and at different temperatures.

KEY WORDS

Hydraulic System, Axial piston pump, RO Desalination, RO membrane, Hydraulic Accumulator, Modeling, Simulation Program, MATLAB, and SIMULINK, Verification.

NOMENCLATURES

A	Membrane permeability coefficient
$A(x_{di})$	Delivery valve throttling area (m^2).
$A(x_{Si})$	Suction valve throttling area (m^2).
A_{di}	Effective area of delivery valve disc (m^2).
A_p	Piston cross section area (m^2).
A_{Si}	Effective area of suction valve disc (m^2).
A_v	Throttle valve throttling area (m^2).
B	Bulks modules of water (kN/m^2).

* Egyptian Armed Forces.

B_e	Equivalent bulks modules of water and hose material (kN/m^2).
B_s	Salt diffusion coefficient.
C_{dd}	Delivery valve discharge coefficient.
C_{dS}	Suction valve discharge coefficient.
C_f	Feed water concentration, (ppm).
C_{fc}	Average concentration of feed-concentrate, (ppm).
C_p	Average permeates concentration, (ppm).
D	Piston diameter, (m).
D_h	Hose diameter (m).
E	Bulks modules of hose material (kN/m^2).
f_{d1}	Delivery valve seat damping coefficient (N.s/m).
f_{d2}	Delivery valve limiter damping coefficient (N.s/m).
f_{di}	Delivery valve moving parts friction coefficient (N.s/m).
F_{Ldi}	Limiter reaction force of delivery valve (N).
F_{LSi}	Limiter reaction force of suction valve (N).
f_{S1}	Suction valve seat damping coefficient (N.s/m).
f_{S2}	Suction valve limiter damping coefficient (N.s/m).
F_{Sdi}	Seat reaction force of delivery valve (N).
f_{Si}	Suction valve moving parts friction coefficient (N.s/m).
F_{SSi}	Seat reaction force of suction valve (N).
H	Head, (m).
h	Hose wall thickness (m).
k	Volumetric losses coefficient, ($\text{m}^5/\text{N.s}$).
k_1, k_2, k_3	Coefficients for a given pump, impeller geometry and speed, (k_1 (m), k_2 (s/m^2), and k_3 (s^2/m^5)).
k_4	The friction coefficient of multi media filter porous media, (N.s/m^5).
k_5	The friction coefficient of multi media filter vessel, ($\text{N.s}^2/\text{m}^8$).
k_6	The friction coefficient of carbon filter porous media, (N.s/m^5).
k_7	The friction coefficient of carbon filter vessel, ($\text{N.s}^2/\text{m}^8$).
k_8	The friction coefficient of cartridge filters element, (N.s/m^5).
k_9	The friction coefficient of cartridge filter vessel, ($\text{N.s}^2/\text{m}^8$).
k_{d1}	Stiffness of moving parts at seat of delivery valve (N/m).
k_{d2}	Stiffness of moving parts at limiter of delivery valve (N/m).
k_{di}	Delivery Valve spring stiffness (N/m).
k_{S1}	Stiffness of moving parts at seat of suction valve (N/m).
k_{S2}	Stiffness of moving parts at limiter of suction valve (N/m).
k_{Si}	Suction valve spring stiffness (N/m).
L	Connecting rod length (m).
m_{di}	Delivery valve disc mass (kg).
m_{Si}	Suction valve disc mass (kg).
n	Pump revolutions per second, (rps).
N_A	The salt flux
N_E	Number of elements in system
n_e	Number of elements in series.
p	Discharge pressure, (Pa).
P_1	Minimum working pressure, (Pa).
P_2	Maximum working pressure, (Pa).
p_{atm}	Atmospheric pressure (Pa).
P_{av}	Pump average pressure, (bar).
p_c	Membrane concentrate pressure, (Pa).

P_{Ci}	Chamber pressure (Pa).
P_{di}	Delivery pressure (Pa).
p_f	Membrane feed pressure, (Pa).
pf	Average concentration polarization factor.
p_{fc}	Average feed-concentrate pressure, (Pa).
P_{max}	Pump maximum pressure, (bar).
P_{min}	Pump minimum pressure, (bar).
P_o	Gas pre-charge pressure, (Pa).
p_p	Permeate pressure, (Pa).
P_{Si}	Suction pressure (Pa).
Q	Flowrate, (m^3/s)
q	Volumetric losses.
Q_{pis}	Piston flowrate, (m^3/s).
Q_a	Accumulator flowrate (m^3/s).
Q_{av}	Pump average flowrate, (m^3/s).
Q_c	System concentrate flowrate, (m^3/s).
Q_d	The piston pump delivery flowrate, (m^3/s).
Q_{di}	Flowrate through delivery valve (m^3/s).
Q_f	System feed flowrate, (m^3/s).
Q_{HPP}	Actual flowrate of the high pressure pump, (m^3/s).
q_L	Internal leakage.
Q_{Li}	Piston leakage flowrate (m^3/s).
Q_{max}	Pump maximum flowrate, (m^3/s).
Q_{min}	Pump minimum flowrate, (m^3/s).
Q_p	Permeate flowrate, (m^3/day).
$Q_{pis i}$	Piston flowrate, (m^3/s).
Q_{pp}	Piston pump flowrate, (m^3/s).
q_{SB}	Leakage through the stuffing box.
Q_s	The piston pump suction flowrate, (m^3/s).
Q_{Si}	Flowrate through suction valve (m^3/s).
q_v	Back flow across the valves.
Q_v	Valve flowrate (m^3/s).
Q_v	Throttle valve flowrate (m^3/s).
r	Radius of the piston pump crank (m).
R_i	Resistance to leakage, ($N.s/m^5$).
s	Piston stroke, (m).
S	Membrane surface area, (m^2).
S_E	Membrane surface area per element, (m^2).
T	Feed water temperature, ($^{\circ}C$).
t	Time (sec).
V	Chamfer initial volume (m^3).
v_p	Piston velocity, (m/s).
V_1	Gas volume at P_1 , (m^3).
V_2	Gas volume at P_2 , (m^3).
V_a	Gas volume in accumulator at P_d , (m^3).
V_{fh}	Water volume at feed water header (m^3).
V_g	Geometric volume, (m^3/rev).
V_h	Water volume inside feed water hose (m^3).
V_L	Volume of the liquid inside the accumulator at P_d , (m^3).
V_{La}	Volume of the liquid entering the accumulator at P_d , (m^3).
V_{Li}	Initial volume of the liquid at the accumulator at P_1 , (m^3).

V_o	Effective gas volume of the accumulator, (m ³).
V_R	Water volume between membrane output and throttle control valve (m ³).
V_T	Water volume from pump output to control valve (m ³).
X_{di}	Displacement of delivery valve spring (m).
X_{dio}	Initial compression distance of delivery valve spring (m).
X_{dm}	Maximum displacement of delivery valve spring (m).
X_{Si}	Displacement of suction valve spring (m).
X_{Sio}	Pre-compression length of suction valve spring (m).
X_{Sm}	Maximum displacement of suction valve spring (m).
Y	System recovery ratio.
Z_i	Displacement of piston (m).
Z_p	Number of Pistons
$\bar{A}(\bar{\pi})$	Average membrane permeability, (m ³ /N. day).
\bar{q}_{fc}	Arithmetic average of feed-concentrate flowrate, (m ³ /s).
$\bar{\pi}$	Average concentrate-side osmotic pressure, (bar).
\bar{Y}_i	Average element recovery ratio.
\bar{R}	Average fractional salt rejection for system
Δp	Pressure drop in membrane, (bar).
Δp_{carf}	Pressure drop across the cartridge filter, (Pa).
Δp_{cf}	Pressure drop across the carbon filter, (Pa).
Δp_{fc}	Pressure drop between feed and concentrate, (Pa).
Δp_{mmf}	Pressure drop across the multi media filter, (Pa).
$\Delta \pi$	Osmotic pressure drop in membrane, (bar).
$\sum m_j$	Summation of all molal concentration of ionic species.
α	Polytropic exponent.
ϵ_P	Pressure irregularity coefficient, (%).
ϵ_Q	Flowrate irregularity coefficient, (%).
η_{vol}	Volumetric efficiency.
θ	The connecting rod angle
ξ_b	Belt slip coefficient.
ξ_m	Electric motor slip coefficient.
ξ_v	Throttle valve hydraulic losses coefficient.
π_f	Feed water osmotic pressure, (bar).
π_p	Permeate-side osmotic pressure, (bar).
ρ	Water density (kg/m ³).
ω	Angular velocity, (rad/s).

INTRODUCTION

Desalination means the removal of fresh water from saline water. Desalination as a natural phenomenon has occurred on earth for millions of years, the natural distillation cycle of water occurs by evaporation of seas and oceans then condensation to form the pure rainwater. This cycle is probably the most obvious example of desalination process (Hanbury, 1993). The other desalination phenomenon that occurs in nature is the freezing of seawater near the polar region. The ice crystals formed are pure water, the salt being excluded from participation in the crystal growth. Desalination has been practiced in the form of distillation for over 2000 years. It is not until the eighteen

century, for people to recognize that the distillation process could be enhanced by cooling the condensing surface.

Many methods have been proposed for desalting saline water, but few were commercially used. The two most popular methods for classifying the well-known desalination processes are as follows:

- Processes **involve phase change**: Vapor-Compression (VC) distillation; Multi-Effect (ME) distillation; Multi-Stage Flash (MSF) distillation,
- Processes **do not involve phase change**: Reverse Osmosis (RO) desalination and Electro-Dialysis (ED) desalination,
- Other processes such as: Ion Exchange; Solar Humidification; and Freezing.

In 1965, the UCLA team installed the first municipal reverse osmosis plant in Coalinga, California. The plant was desalting water containing 2,500 ppm (part per million) salts, to producing about 20 m³ /day with a tubular cellular acetate membrane. The development of the tubular, spiral-wound, and hollow-fine-fiber modules together with the development of the polyamide membranes took place from 1965-1970. Through the 1980s, improvements were made to these membranes to increase water flux and salt rejection with both brackish water and seawater. Brackish water is water that contains dissolved matter at an approximate concentration ranges from 1,000 - 5,000 ppm. Seawater distillation plants dominated the early desalination planets. However, due to lower energy requirements, a desalination process called reverse osmosis, RO, now appears to have a slightly lower cost than distillation for seawater desalination. For brackish water desalination, RO and another desalination process called electro-dialysis, ED, are both competitive. Other desalination technologies are less widely used due to their rudimentary development and/or higher cost. However, there is no single desalination technology that is considered “best” for all uses. The selection of the most appropriate technology depends on the composition of the feed water (prior to desalination), the desired quality of the product water, and many other site-specific factors (Al-Shayji, 1998). Permeate flux and salt rejection is the key performance parameters of a reverse osmosis process, where, permeate flux is the rate of permeate transported per unit of membrane area measured in liter per square meter per hour (liter/m².h). Salt rejection is the percentage of solids concentration removed from system feed water by the membrane. Permeate flux and salt rejections are mainly influenced by varying the following operation parameters: pressure, temperature, recovery, pH, and feed water salt concentration.

In this paper, simulation of RO seawater desalination system is introduced to investigate the dynamic behavior of the high pressure pump and the performance of the RO membrane.

MATHEMATICAL MODELING AND SIMULATION

To simulate the operation of a water desalination plant of RO process, a mathematical model has to be developed. The governing equations, which characterize the performance of RO system components, have to be investigated. The components of RO plant under study are shown in Fig. 1. It consists of a pre-treatment unit and a high pressure unit.

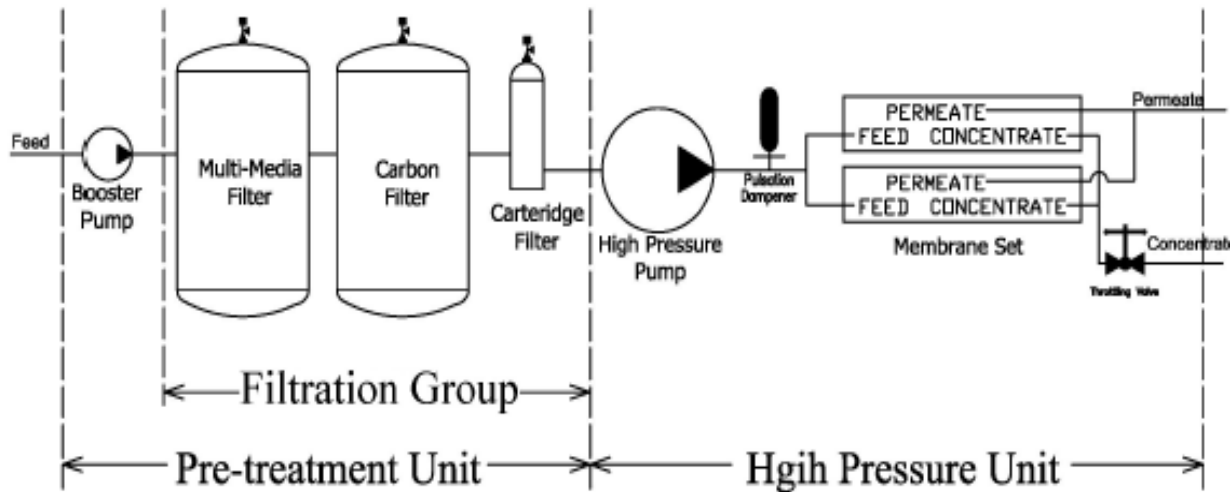


Fig. 1 Components of pre-treatment and high pressure units.

Equation which describe each component will be presented separately. The simulation program is the result of combining all derived mathematical equations to form a complete simulation model for the sea water desalination plant.

Mathematical Model of Pre-Treatment Unit

It consists of a booster pump of centrifugal type at which its head depends on the delivered flowrate at constant revolutions, and a filtration group that consists of three filters (multi-media filter, activated carbon filter, and cartridge filter). The booster pump characteristic equation (Euler's head versus flowrate) is developed from the energy equation by considering the effect of using finite number of vanes, as well as the effect of hydraulic losses in the flow passages (Cherkassky, 1985) and (Stepanoff, 1967).

Characteristic equation of the booster pump

The pump is of fixed impeller geometry working at constant speed; its characteristics expressed in the following form:

$$H = k_1 - k_2Q - k_3Q^2$$

Detailed description of the pump characteristic equation and its coefficients are presented in Ref. (Seoudy, 2003), App. (A-1). Characteristic curves and technical specifications of the booster pump introduced by the manufacturer are presented in Ref. (Seoudy, 2003), App. (B-1). The pump characteristic equation has been obtained by the curve fitting technique (at operation revolutions of 2900 rpm) as follows:

$$H = 50.152 + 0.1698 \times Q - 0.0103 \times Q^2$$

Characteristic equation of filtration group

The delivered head and flowrate of the booster pump are the input parameters to the filtration group. The characteristics equations of filters expressed in the following forms:

For multi-media filter: $\Delta p_{mmf} = k_4 \times Q + k_5 \times Q^2$

For activated carbon filter: $\Delta p_{cf} = k_6 \times Q + k_7 \times Q^2$

For cartridge filter: $\Delta p_{carf} = k_8 \times Q + k_9 \times Q^2$

Detailed description of the filters characteristic equations and their coefficients are presented in Ref. (Seoudy, 2003), App. (A -2).

Mathematical Model of High Pressure Unit

The high pressure unit consists of the high pressure pump, and the RO membrane. The installed high pressure pump in the RO plant is of piston type, and RO membrane is of spiral wound type.

Characteristic equation of the high pressure pump

The high pressure pump is a positive displacement pump of axial piston type. The reciprocating motion of the piston gives fluctuating flowrate and pressure. The pistons are the main source of flow fluctuations which is due to the overlaps of fluid discharge from more than one piston into a single exit port of the pump. Fig. 2. shows one of the pump cylinders which includes piston, stuffing box, inlet and outlet valves, and manifolds, (Wheatly, 1996). Detailed description of the piston pump, technical specifications and main dimensions of the pump used in the RO desalination plant are introduced in Ref. (Seoudy, 2003), App. (B-2).

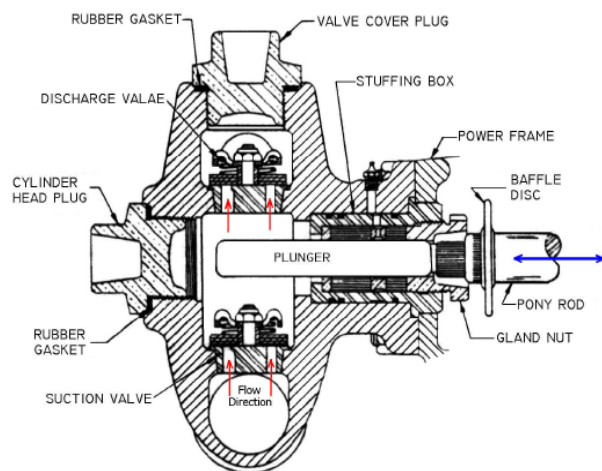


Fig. 2 Cross-section of one cylinder of piston pump.

The input flow rate of high pressure pump equals the exit flowrate from the filters. The characteristic equation which represents the flowrate of the pump may be determined as given in Cherkassky, 1985, and Karassik, 1999 as follows:

$$Q_{pp} = V_g \times n \times \xi_m \times \xi_b \eta_{vol} \text{ where, } V_g = \frac{\pi}{4} D^2 \times s \times z_p$$

Performance characteristic of the piston pump depends on many independent parameters. The most important parameters is the *volumetric losses*, which is affected by: leakage, incomplete filling, aeration, and cavitation. When handling liquids of low-viscosity, there are volumetric losses in the pump delivery due to leakage between the stationary and moving parts. The actual pump capacity at any particular pump speed and fluid viscosity is the difference between the theoretically displaced volume and the losses due to leakage. Viscosity, μ , pressure, p , clearances, c , and speed, n , are the major factors that influence volumetric losses. Pump volumetric losses are function of $(p.c^3 / \mu)$, incomplete filling, and cavitations effect, (Karassik, 1999). The pump operates with a positive pressure in the suction line, therefore assuming complete filling of the pump, and no cavitation occurrence. The volumetric losses could be expressed as introduced in (Karassik, 1999) as follows:

$$q = q_{SB} + q_V + q_L$$

Volumetric losses could be expressed as a percentage of the suction capacity. The pump delivery flowrate at an operating point is a function of the suction flowrate and the operating pressure. Then the characteristic equation that represents the piston pump performance could be written as:

$$Q_{HPP} = Q_{pp} - k \cdot p$$

In order to study the dynamic performance of the high pressure pump, the equations governing the fluid motion inside the piston chamber should be derived. The piston chamber is composed of four parts, the piston, the suction valve, the delivery valve, and the chamber, as shown in Fig. 3.

a) Piston:

The pump flow rate for five pistons results from the superposition of the volume rate of liquid drawn by each piston with $(2\pi/5)$ angle shift for each piston,

$$Q_{pis_j} = A_p r \omega \sin\left(\omega t + \frac{(j-1)}{z_p} 2\pi\right)$$

Where: $J = 1-5$

The total pump flowrate $Q_{hpp} = \sum_{j=1}^5 Q_{pis_j}$

b) Suction valve:

- **The flowrate through the suction valve**

$$Q_{Si} = C_{dS} A(x_{Si}) \sqrt{\frac{2(P_{Si} - P_{Ci})}{\rho}} \quad A(x_{Si}) = x_{Si} \times \pi d_s$$

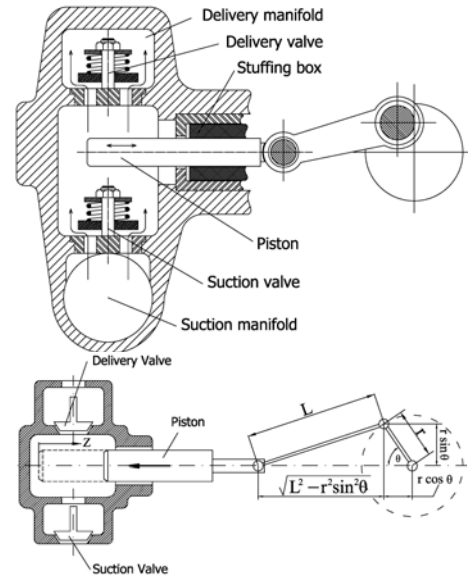


Fig. 3 Piston chamber of the high pressure pump

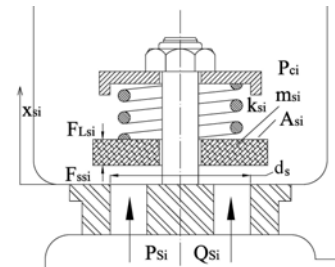


Fig. 4 Suction Valve

The pump suction flowrate through the suction valve equals to the superposition of flowrates through the individual suction valves:

$$Q_S = \sum_{i=1}^5 Q_{Si}$$

- **Equation of motion of moving parts**

$$m_{Si} \ddot{x}_{Si} + f_{Si} \dot{x}_{Si} + k_{Si} (x_{Sio} + x_{Si}) = (P_{Si} - P_{Ci}) A_{Si} + F_{Ssi} - F_{LSi}$$

- **Seat and limiter reaction forces**

The moving parts move up and back to the valve seat following the change in pressure fluctuations. At the valve seat the direction of the motion is limited mechanically by the

valve body material and results in development of a counter seat reaction force. The seat reaction force could be written as follow:

$$F_{SSi} = \begin{cases} 0 & x_{Si} > 0 \\ k_{S1}x_{Si} + f_{S1}\dot{x}_{Si} & x_{Si} \leq 0 \end{cases}$$

At the other direction of motion the valve is limited mechanically by a limiter, the limiter reaction force could be written as follow:

$$F_{LSi} = \begin{cases} k_{S2}(x_{Si} - x_{Sm}) + f_{S2}\dot{x}_{Si} & (x_{Si} - x_{Sm}) \geq 0 \\ 0 & (x_{Si} - x_{Sm}) < 0 \end{cases}$$

c) Delivery valve:

• **Flowrate through the valve**

$$Q_{di} = C_{dd} A(x_{di}) \sqrt{\frac{2(P_{Ci} - P_{di})}{\rho}} A(x_{di}) = x_{di} \times \pi d_d$$

The pump delivery flowrate is given by: $Q_d = \sum_{i=1}^5 Q_{di}$

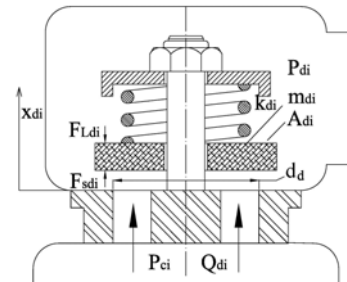


Fig. 5 Delivery Valve

• **Equation of motion of moving parts:**

$$m_{di} \ddot{x}_{di} + f_{di} \dot{x}_{di} + k_{di} (x_{dio} + x_{di}) = (P_{Ci} - P_{di}) A_{di} + F_{Sdi} - F_{Ldi}$$

• **Seat and limiter reaction forces:**

The delivery valve seat reaction force could be written as follow:

$$F_{Sdi} = \begin{cases} 0 & x_{di} > 0 \\ k_{d1}x_{di} + f_{d1}\dot{x}_{di} & x_{di} \leq 0 \end{cases}$$

where: k_{d1} : Stiffness of moving parts at seat of delivery valve (N/m); f_{d1} : Delivery valve seat damping coefficient (N.s/m).

The limiter reaction force could be written as follow:

$$F_{Ldi} = \begin{cases} k_{d2}(x_{di} - x_{dm}) + f_{d2}\dot{x}_{di} & (x_{di} - x_{dm}) \geq 0 \\ 0 & (x_{di} - x_{dm}) < 0 \end{cases}$$

where: x_{dm} : Maximum displacement of delivery valve spring (m); k_{d2} : Stiffness of moving parts at limiter of delivery valve (N/m); f_{d2} : Delivery valve limiter damping coefficient (N.s/m).

d) Piston chamber:

• Continuity equation applied to piston chamber:

The continuity equation applied to the control volume CV1 in the piston chamber as shown in Fig. 6 could be written as follow:

$$A_p \dot{z}_i + Q_{Si} - Q_{di} - Q_{Li} = \frac{(V - A_p z_i)}{B} \frac{dP_{ci}}{dt}$$

$$Q_{Li} = \frac{P_{ci} - P_{atm}}{R_i}$$

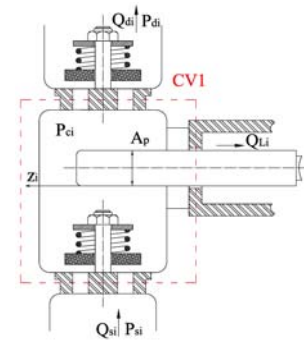


Fig. 6 Piston Chamber

e) Characteristic equation of the accumulator

A diaphragm accumulator utilizes a gas (nitrogen) in storing the hydraulic energy. The diaphragm accumulator is charged by the water from the hydraulic circuit when its pressure increases and thus, compresses the gas side of accumulator. It discharges the water to the circuit when its pressure decreases by the expansion of the gas. Fig. 7 shows the accumulator assembly.

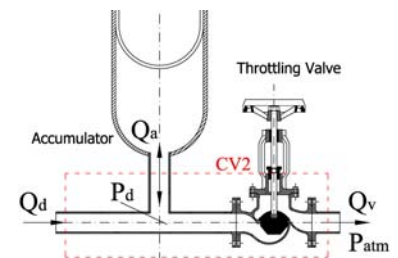


Fig. 7 Control volume around accumulator and throttle valve

• Continuity equation applied to the accumulator:

The continuity equation applied to the control volume CV2 as shown in Fig. 11, could be written as follow:

$$Q_d - Q_v = Q_a$$

• Ideal gas law

The diaphragm accumulator may be considered to follow the ideal gas laws. Fig. 8 shows the working phases (a) precharged, (b) minimum working pressure, (c) working pressure, and (d) maximum working pressure. The state equation (ideal gas law) applied on the accumulator, assuming isothermal polytropic process, could be written as follow:

$$P_o \times V_o^\alpha = P_1 \times V_1^\alpha = P_d \times V_a^\alpha = P_2 \times V_2^\alpha$$

• Accumulator flowrate, Qa

The accumulator flow rate could be written as follows:

$$Q_a = \frac{dV_{La}}{dt} \quad ; \quad V_L = V_{Li} + V_{La} \quad ;$$

$$V_{Li} = V_o - V_1 \quad ; \quad V_a = V_o - V_L$$

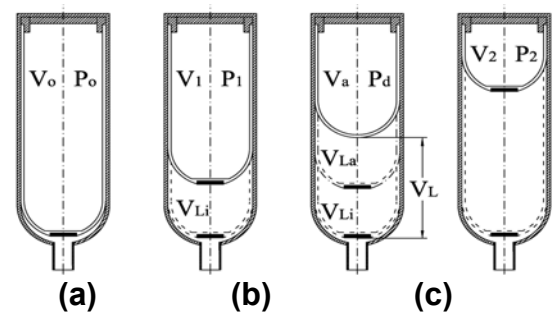


Fig. 8 Accumulator working phases

f) Characteristic equation of the throttle valve

Throttling valve is used to control the pump delivery pressure. Fig. 9 shows the throttle valve assembly.

- **Flow rate through throttle valve**

$$Q_v = \frac{A_v}{\sqrt{\xi_v}} \sqrt{\frac{2(p_d - p_{atm})}{\rho}}$$

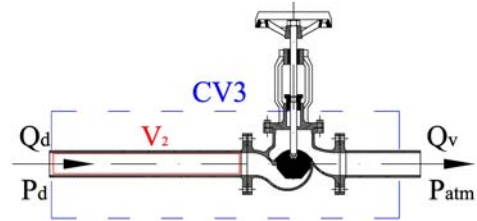


Fig. 9 Throttling valve control volume

- **Continuity equation applied to the throttle valve**

$$Q_d - Q_v = \frac{V_T}{B} \frac{dP_d}{dt}$$

g) Characteristic equation of the feed header and membrane

The feed header distributes the feed water from the high pressure pump to the membrane. The feed water is divided inside the membrane into two passes, the 1st is the permeate water pass and the 2nd is the concentrate water pass. The equations that describe the feed header and membrane could be written as follows:

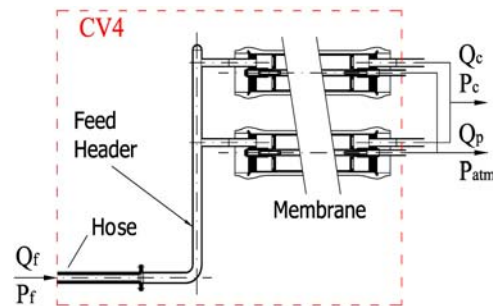


Fig. 10 Feed header and membrane Control volume

- **Continuity equation applied to feed header and membrane:**

The continuity equation applied to the control volume CV4 as shown in Fig. 10 could be written as follows:

$$Q_f - Q_c - Q_p = \left(\frac{V_h}{B_e} + \frac{V_{fh}}{B} \right) \frac{dP_f}{dt} \quad \text{and} \quad B_e = \frac{1}{1/B + 5D_h/4Eh}$$

The pressure loss in feed header may be considered as local losses type. The losses in pressure could be neglected w.r.t. the operating pressure of the system.

R.O. Membrane

The pump exit flowrate enters the membrane unit and exits in two passes, the permeate flowrate and the brine (concentrate) flowrate. Construction of a single membrane element is shown in Fig. 11. Detailed manufacturing description, water flow directions, technical specifications, and main dimensions of the membrane element used in water desalination plant are introduced in Ref. (Seoudy, 2003), App. (B-3).

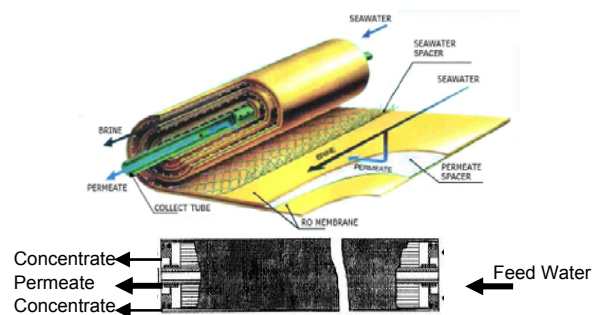


Fig. 11 Construction of a single membrane element

The membrane elements are arranged as two parallel elements with two series elements for obtaining the most water treatment performance. Each two series element is placed in one pressure vessel as shown in Fig. 12. The performance of a specified R.O. membranes are defined by the feed pressure, or by the permeate flow if the feed pressure is specified, and by the salt passages.



Fig. 12 Arrangement of membrane elements

In simplest terms, the permeate flow Q_p through an R.O. membrane is directly proportional to the wetted surface area, S , times the net permeation driving force ($\Delta p - \Delta \pi$) (Dow, 1995). The proportionality constant is the membrane permeability coefficient. Fig. 13 shows the pressure distribution in the membrane and how it affects the permeate flowrate. The membrane performance is the total system

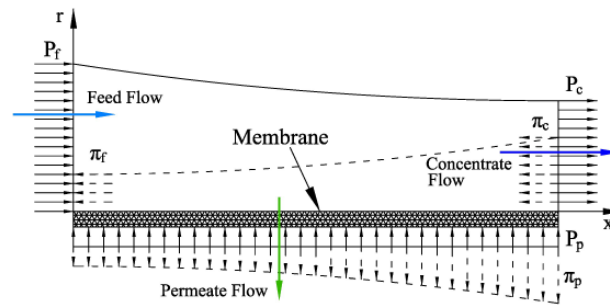


Fig. 13 Pressure distribution in R.O. membrane

permeate flowrate equation which including number of correction factors, such as:

- Temperature correction factor for membrane permeability, TCF ,
- Membrane fouling factor, FF ,
- Number of elements in system, N_E ,

a) The permeate flowrate equation, (Dow, 1995), will be introduced as follows:

The permeate flowrate out of the membrane is given by the following equation:

$$Q_p = N_E \times S_E \times \bar{A}(\bar{\pi}) \times TCF \times FF \times \{\Delta p - \Delta \pi\}$$

The detailed determination of the driving pressure, the average membrane permeability, the temperature correction factor, and the fouling factor for a differential element, is introduced in Ref. (Seoudy, 2003).

b) Concentrate flowrate

The concentrate flowrate out of the membrane could be calculated from the following:

$$Q_c = 2 \times \left(\frac{P_f - P_c}{0.01 \times n_e} \right)^{1/1.7} - Q_f$$

Reject header and throttling valve

The rejection header collects the reject water from the output (high pressure side) of the membrane to pass through the throttling valve. The throttling valve controls the feed pressure at the membrane entrance. The equations that describe the reject header and throttling valve could be written as follows:

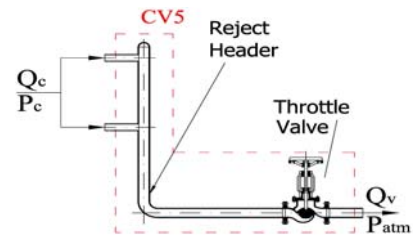


Fig. 14 Reject header and throttling valve control volume

- **Continuity equation applied to reject header and throttling valve:**

The continuity equation for the reject header and throttling valve applied to the control volume CV5 as shown in Fig. 14 could be written as follow:

$$Q_c - Q_v = \frac{V_R}{B} \frac{dP_c}{dt}$$

- **Flow rate through throttling valve**

The delivery flowrate exit from the membrane enters into the throttle valve. The throttle valve flowrate could be written as follow:

$$Q_v = \frac{A_v}{\sqrt{\xi_v}} \sqrt{\frac{2(P_C - P_{atm})}{\rho}}$$

The pressure loss in reject header may be considered a local loss which could be neglected relative to the operating pressure of the system.

A simulation program has been developed based on the above mentioned equations by using SIMULINK 4 in MATLAB 6.1 computer program shown in figures below from Fig. 15 to Fig. 19 which simulates the characteristic of the high pressure pump loaded by the membrane. The detailed description of this program is introduced in Ref. (Seoudy, 2003), App. (E-3). The obtained model for the desalination plant components should be validated by experimental measurements on real RO plant. Part 2 of this paper encloses the experimental measurements on a real RO plant and the theoretical study of plant performance through the validated simulation program.

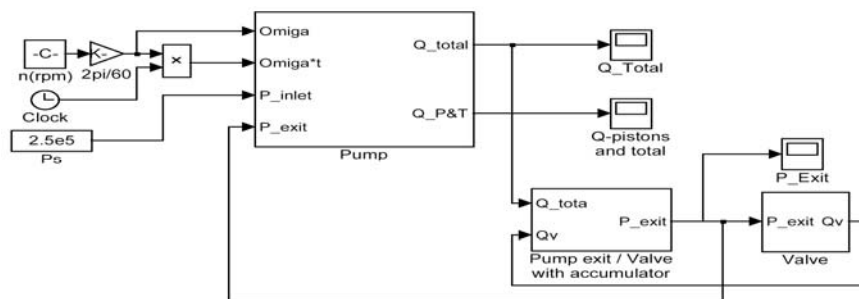


Fig. 15 High pressure components.

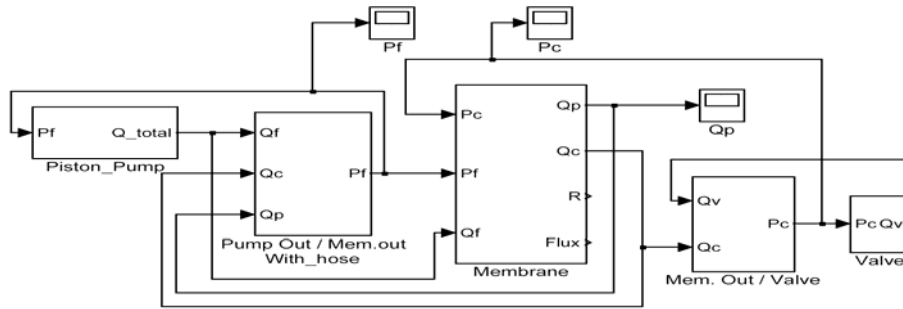


Fig. 16 The high-pressure pump loaded by membrane.

Max. step size= 0.001 & Relative tolerance = 0.001 & Solver: ode 23s (stiff/Mod. Rosen Brock)

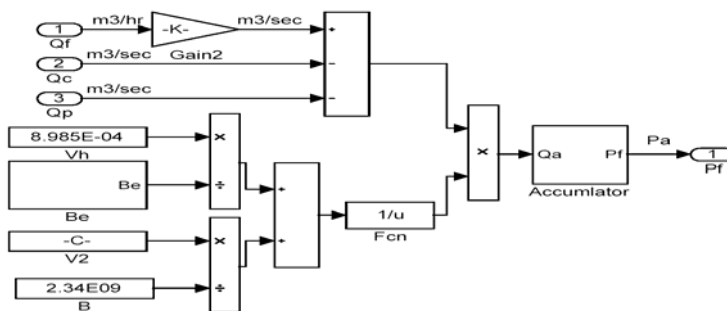


Fig. 17 Continuity equation between the pump and throttling valve (without accumulator).

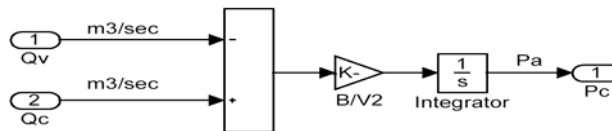


Fig. 18 Continuity equation between the membrane and throttling valve.

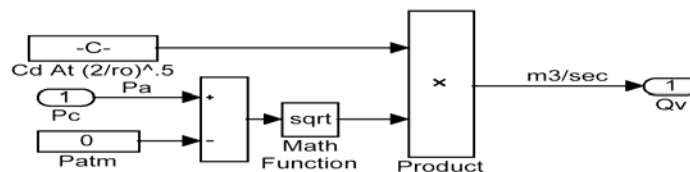


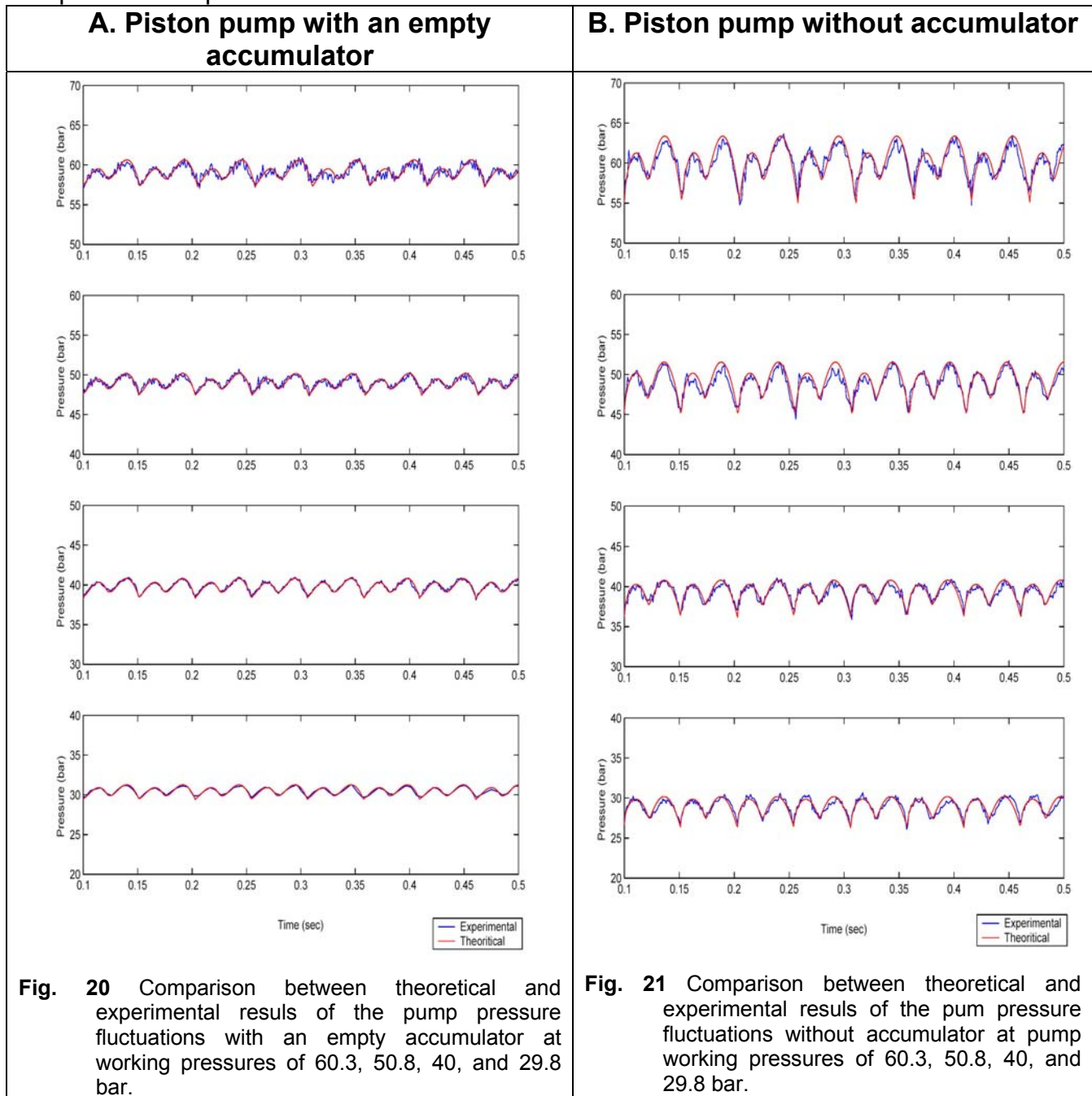
Fig. 19 Flow rate through the throttling valve.

VALIDATION OF PLANT SIMULATION MODEL

To validate the programmed simulation model of RO plant including a high pressure piston pump and RO membranes, the theoretical results have been compared with experimental measurements on a real desalination plant (introduced in part 2 of this paper) beside some published results for RO membranes.

Validation of Piston Pump Simulation Program

The piston pump pressure fluctuations have been determined theoretically from the developed simulation program and compared with the corresponding experimentally measured pressure fluctuations at different pump operating pressures. The pressure signal frequencies and amplitudes are almost the same at all pump pressures as shown in Fig. 20 and Fig. 21. The experimental signal has ripples; this may be related to fluid flow throughout, pipes (fixation, connections), and other mechanical elements. Comparison between the experimental and the theoretical results for different cases of operation are presented as follows:



Therefore, the derived simulation models could be used for more theoretical investigations for the pump behavior at proposed conditions to save practical investigation costs and time.

Validation of RO Membrane Simulation Program

The validation of the RO membrane simulation program has been done by comparing the present theoretical results of simulation program with both of experimental work introduced in part 2 of this paper and of some published results as follow:

A. Comparison of simulation and experimental work

Figures from 22 to 24 show the comparison of the permeate flowrate and salt rejection results from the present theoretical model and from the experimental measurements of the three different salinities (21000 ppm, 28900 ppm, and 33000 ppm). The experiments have been performed at feed pressures ranges from 30 to 65 bar using two by two arrangements of membrane, Film Tec SW30HR-380 elements; seawater spiral wound membrane.

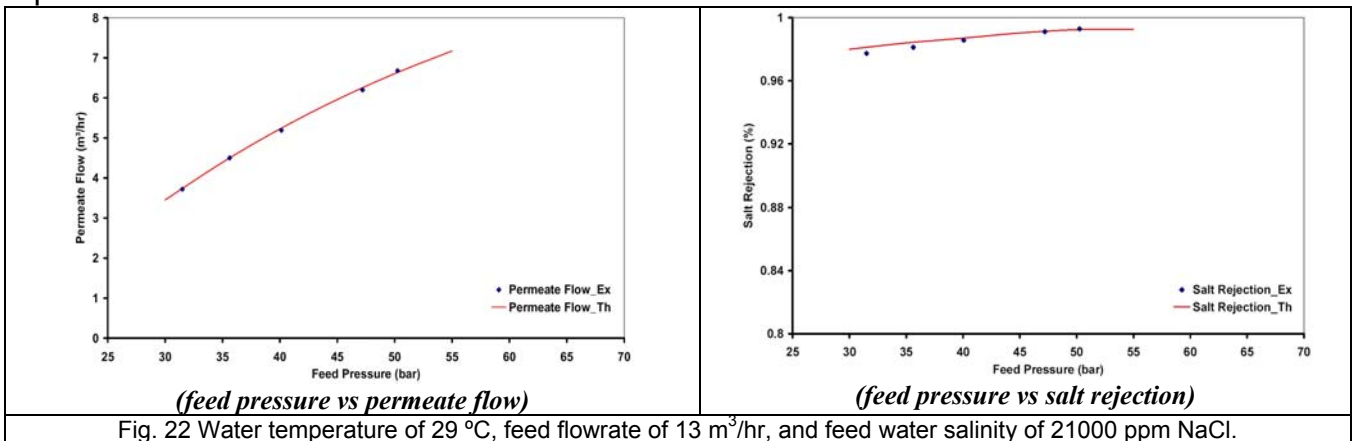


Fig. 22 Water temperature of 29 °C, feed flowrate of 13 m³/hr, and feed water salinity of 21000 ppm NaCl.

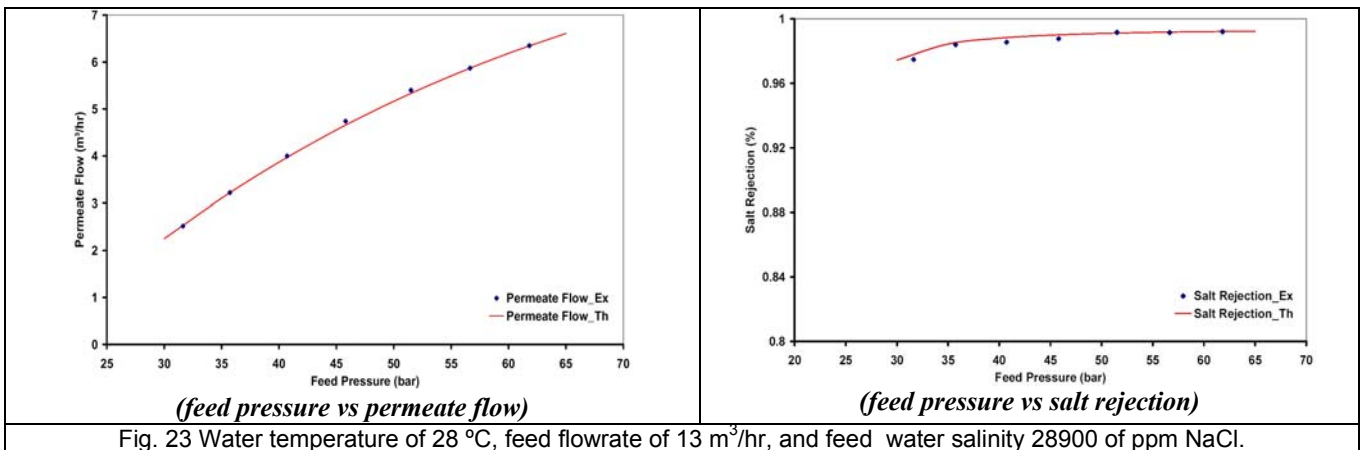


Fig. 23 Water temperature of 28 °C, feed flowrate of 13 m³/hr, and feed water salinity 28900 of ppm NaCl.

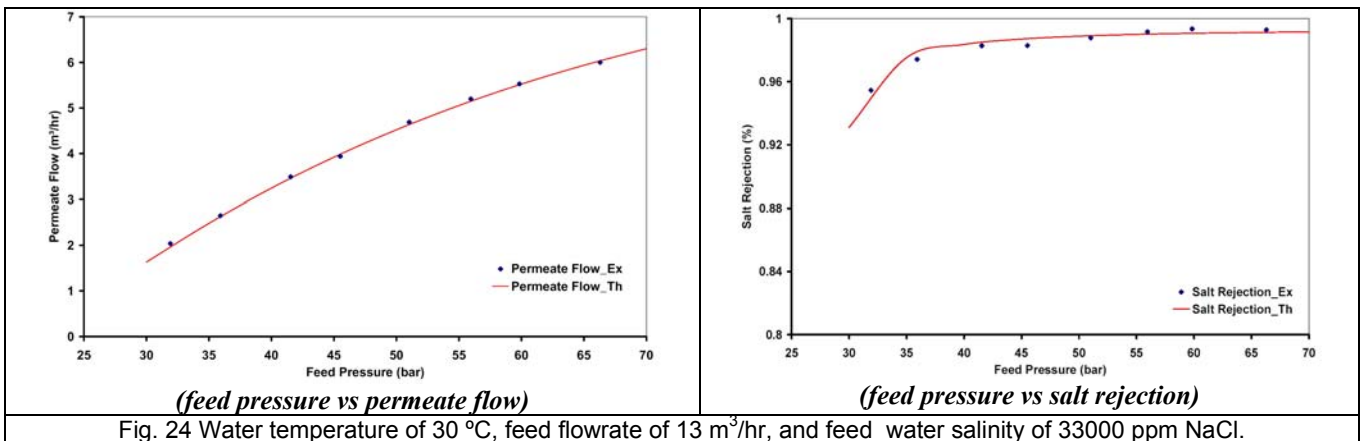


Fig. 24 Water temperature of 30 °C, feed flowrate of 13 m³/hr, and feed water salinity of 33000 ppm NaCl.

B. Comparison of simulation and some published results

The results of the theoretical model discussed earlier for the spiral-wound membrane along with the experimental results by (Al-Bastaki and Abbas, 2000), and membrane Tech. Manual (Dow, 1995):

Fig. 25 shows the comparison of the permeate flowrate results from the present theoretical model along with the experimental results of Al-Bastaki and Abbas, 2000. The experiments were performed at different inlet pressures (from 20 to 50 bars) using a single element Film Tec SW30-2521-A seawater spiral wound membrane. The feed water was prepared by mixing sodium chloride in distilled water. All the experiments were performed at a temperature of 25°C and a feed concentration of 10,000 ppm. A more detailed description of the tested membrane element and its constants used in the model are presented in Ref. (Seoudy, 2003), App. F.

Fig. 26 shows the comparison of the permeate flux and salt rejection results from the present theoretical model along with the experimental results given in the membrane Tech. Manual (Dow, 1995). The experiments were performed at different inlet pressures (from 27 to 69 bar) using a single element FilmTec SW30-8040-A seawater spiral wound membrane. The feed water was prepared by mixing sodium chloride in distilled water. All the experiments were performed at a temperature of 25°C and a feed concentration of 35,000 ppm. A more detailed description of the tested membrane element and its constants used in the model are presented in Ref. (Seoudy, 2003), App. G.

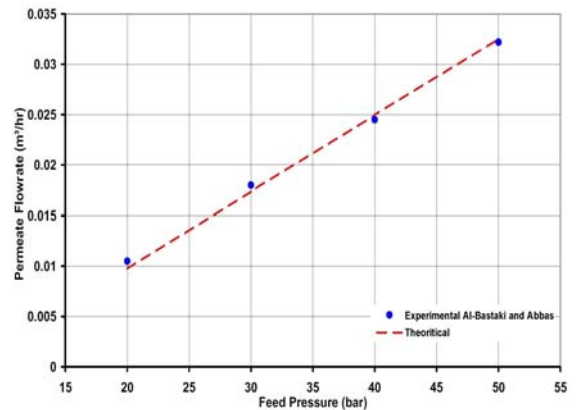


Fig. 25 Comparison of the permeate flowrate results from the present theoretical investigation along with the experimental results of Al-Bastaki and Abbas, 2000.

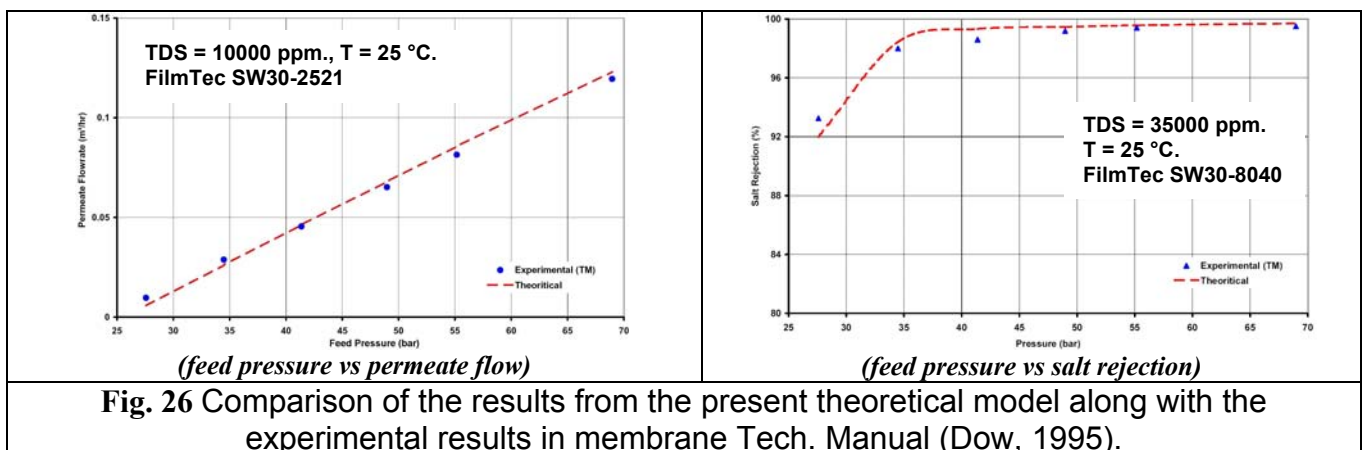
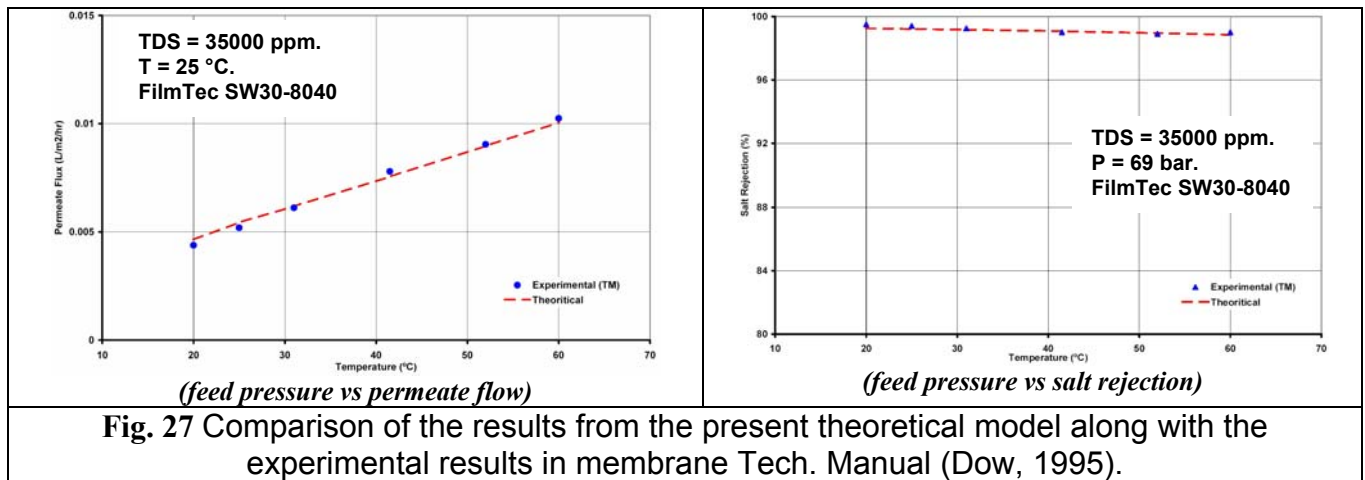


Fig. 26 Comparison of the results from the present theoretical model along with the experimental results in membrane Tech. Manual (Dow, 1995).

Fig. 27 shows the comparison of the permeate flux and salt rejection results from the present theoretical model along with the experimental results given in the membrane Tech. Manual (Dow, 1995). The experiments were performed at different temperatures (from 20 to 60 °C) using a single element FilmTec SW30-8040-A seawater spiral wound membrane. All the experiments were performed at a pressure of 69 bar and a feed concentration of 35,000 ppm. These figures show good agreement between the manufacturer and theoretical results.



The figures from Fig. 25 to Fig. 27 show good agreement between the theoretical results from simulation model and the experimental from published results, which implies the validation of the simulation model.

CONCLUSION

The constructed simulation program of the RO desalination plant is verified and could be used for theoretical investigations which save time and cost such as:

- Prediction of the effect of any operating parameter change (salinity, water temperature, pump pressure or flowrate, membrane type, ...etc.) on the plant performance,
- Optimization operating parameters,
- Trouble shooting of RO plant.

Part 2 of this paper encloses the experimental measurements on a real RO plant and the theoretical investigations on the validated simulation model.

REFERENCES

1. Al-Bastaki, N. M., and Abbas, A., "Predicting the Performance of RO Membranes", Conference On Membranes In Drinking and Industrial Water Production, L'Aquila, Italy, Vol. 2, pp 397–403, October 2000.
2. Al-Shayji, Khawla Abdulmohsen, "Modeling, Simulation, and Optimization of Large-Scale Commercial Desalination Plants", Ph.D thesis, Virginia Polytechnic Institute and State University, USA, 1998.
3. Cherkassky, V.M., "Pumps, Fans and Compressors", Mir Publishers, Moscow, 1985.
4. Dow Chemical Company "FILMTEC Membrane" Technical Manual, April 1995.
5. Etsion, I., and Magen, M. "Piston Vibration in Piston-Cylinder Systems", Transaction of the ASME Journal of Fluid Engineering, Vol, 87, pp 214-221, March.1980.
6. Goulds Pump Company "Technical Manual", USA, 1998.

7. Hanbury, W.T., Hodgkiess, T., and Morris, R., "Desalination Technology", Intensive Course Manual, Porthan Ltd.- Easter Auchinloch, Glasgow, UK 1993.
8. Harris, R. M., Edge, K. A., And Tilley, D. G., "The Suction Dynamics of Positive Displacement Axial Piston Pumps" Transaction of the ASME Journal of Dynamic System, Measurement and Control, Vol. 116, No. 1, pp 281-287, 1994.
9. Karassik, I. J., Messina, J. P., Cooper, P., Heald, C. C., "Pump Hand Book", Third Edition , JON WILEY & SONS, INC., 1999.
10. Nakano, H. , Machiyama, T., and Kawase, T. "Modelling of the Generation Mechanism of Flow Pulsation's by an Axial Piston Pump" Bulletin of the JSME, Vol. 26, No. 175, pp. 203-208, 1986.
11. Seoudy, A., "Simulation of R.O. Seawater Desalination System", M.Sc. thesis, Military Technical College, Cairo, Egypt, 2003.
12. Stepanoff, A.J., "Centrifugal and Axial Flow Pumps", John Wiley, New York, 1967.
13. Taniguchi, M., Kurihara, M., and Kimura, S., "Behavior of a Reverse Osmosis Plant Adopting a Brine Conversion Two-Stage Process and Its Computer Simulation", Journal of Membrane Science, Vol. 183, pp 249–257, 2001.
14. Wheatly Gaso Inc. "wheatly Pumps" Operator's Manual, USA, 1996.